Submitted to

**XVII International Workshop on Deep Inelastic Scattering and Related Subjects, DIS2009**, April 26-30, 2009, Madrid, Spain.

*Electronic Access: www-h1.desy.de/h1/www/publications/H1preliminary.short_list.html*
*www-zeus.desy.de/physics/phch/conf/dis09/index.html*

H1prelim-09-064
ZEUS-prel-09-008
April 2009

# Multi-Leptons with High Transverse Momentum at HERA

The H1 and ZEUS Collaborations

**Abstract**

Events with at least two high transverse momentum leptons (electrons or muons) are studied using the full $e^{\pm}p$ data sample collected by the H1 and ZEUS experiments at HERA. The data correspond to an integrated luminosity of $0.94$ fb$^{-1}$. The observed numbers of events are in good agreement with the Standard Model predictions. Seven di- and tri-lepton events are observed in $e^{+}p$ collision data with a scalar sum of the lepton transverse momenta above 100 GeV, while $1.94 \pm 0.17$ such events are expected. No event is seen in $e^{-}p$ collisions in this region for $1.19 \pm 0.12$ expected. The data are used to measure total and differential di-electron and di-muon production cross sections in a restricted phase space dominated by photon-photon collisions.

# 1 Introduction

Within the Standard Model (SM) the production of multi-lepton final states in electron[1]-proton collisions proceeds mainly via photon-photon interactions [1]. At high transverse momenta, the clean experimental signature along with the small and precisely calculable production cross section offer a high sensitivity to searches for contributions from beyond the SM [2]. Measurements of multi-lepton production at the HERA collider have already been performed by the H1 [3–5] and ZEUS [6] Collaborations using data samples corresponding to an integrated luminosity of up to $\sim 0.5$ fb$^{-1}$. Events with high invariant mass $M_{12}$ of the two highest $P_T$ leptons or high scalar sum of lepton transverse momenta $\sum P_T$ were measured by both experiments in a region where the SM expectation is low.

In order to minimise statistical uncertainties in the measurement of these rare multi-lepton topologies, a combination of H1 and ZEUS results which exploits the complete $e^{\pm}p$ data samples of both experiments has been performed and is presented in this paper. Total yields and kinematic distributions of multi-lepton final states with electrons or muons are measured and compared to the SM predictions. The two-fold increase in the available data statistics allows a more stringent test of the SM in the high mass and high $\sum P_T$ regions. In addition, combined total and differential cross sections of the production of $e^+e^-$ and $\mu^+\mu^-$ pairs are measured in a restricted phase space region dominated by photon-photon collisions and with an improved statistical accuracy compared to previous publications [5, 6].

# 2 Experimental Conditions

The analysed data were collected between 1994 and 2007 at the HERA electron-proton collider using the H1 and ZEUS detectors. The data are recorded at electron and proton beam energies of $27.6$ GeV and $820$ GeV or $920$ GeV, corresponding to centre-of-mass energies $\sqrt{s}$ of $301$ GeV or $319$ GeV, respectively. The total integrated luminosity of the data is $0.94$ fb$^{-1}$. The data comprise $0.38$ fb$^{-1}$ recorded in $e^-p$ collisions and $0.56$ fb$^{-1}$ in $e^+p$ collisions, of which $8\%$ were recorded at $\sqrt{s} = 301$ GeV.

The H1 and ZEUS detectors are general purpose instruments which consist of a charged particle tracking system in a magnetic field surrounded by electromagnetic and hadronic calorimeters and muon detectors, ensuring a hermetic coverage around the $ep$ interaction point. The origin of the H1 and ZEUS coordinate systems is their respective nominal $ep$ interaction point, with the direction of the proton beam defining the positive $z$-axis (forward region). The transverse momentum is measured in the $x - y$ plane. The pseudorapidity $\eta$ is related to the polar angle $\theta$ by $\eta = -\ln\tan(\theta/2)$. Detailed descriptions of the H1 and ZEUS detectors can be found elsewhere [7, 8].

The SM predicts that isolated multi-lepton final states are mainly produced by photon-photon interactions, $\gamma\gamma \to \ell^+\ell^-$. The GRAPE [9] Monte Carlo (MC) event generator was used to simulate this process and calculate SM production cross sections. GRAPE predicts

[1]Here and in the following, the term "electron" denotes generically both the electron ($e^-$) and the positron ($e^+$).

cross sections for $ep \rightarrow e\,\mu^+\mu^- X$ and $ep \rightarrow e\,e^+e^- X$ processes, leading to $e\mu\mu$ and $eee$ final states. Events with only two leptons ($\mu\mu$, $e\mu$ or $ee$) are observed if the scattered electron or one lepton of the pair is not detected. The $ep \rightarrow e\,\tau^+\tau^- X$ process with subsequent leptonic tau decays is also simulated with GRAPE and its contribution to the studied final states is found to be at most $4\%$.

Experimental backgrounds to $ee$ and $eee$ final states arise from events in which, in addition to a genuine electron, one or two fake electrons are reconstructed. Neutral current (NC) deep-inelastic scattering (DIS) events ($ep \rightarrow eX$) in which hadrons or radiated photons are wrongly identified as electrons constitute the dominant background contribution. QED Compton (QEDC) scattering $ep \rightarrow e\gamma X$ may also contribute if the photon is misidentified as an electron. Background to the $e\mu$ final state may arise from NC DIS events if hadrons are misidentified as muons.

# 3 Event selection

For this analysis, a common phase space region was chosen according to the individual performances of the H1 and ZEUS detectors, such that both detectors have high and well understood acceptance. It is slightly smaller than the ones used in [5] and [6] and is described in the following.

Electron candidates are identified in the polar angle range $5^\circ < \theta < 175^\circ$ as a compact and isolated energy deposit in the electromagnetic calorimeters. The electron energy threshold is $10$ GeV in the polar angle range $5^\circ < \theta < 150^\circ$ and $5$ GeV in the backward region ($150^\circ < \theta < 175^\circ$). Compared to the published H1 analysis [5], the electron energy threshold is here raised in the central region ($20^\circ < \theta < 150^\circ$) from $5$ to $10$ GeV. Muon candidates are identified in the polar angle range $20^\circ < \theta < 160^\circ$ with a minimum transverse momentum of $2$ GeV. Muon identification is based on the measurement of a track in the inner tracking system associated to a track segment reconstructed in the muon chambers or an energy deposit in the calorimeter compatible with a minimum ionising particle. Detailed descriptions of electron and muon identification criteria used by the H1 and ZEUS experiments are given in the previous publications [5, 6]. For the H1 experiment, the resulting electron identification efficiency is $80\%$ in the central region and larger than $95\%$ in the forward and backward regions, while for the ZEUS detector the electron identification efficiency is of about $90\%$. The lower electron identification efficiency in H1 analysis is mainly due to a tight matching requirement between the transverse momenta measured by the tracker and the calorimeter. It allows to strongly reduce the electron mis-identification in $ee$ final states [3, 5]. The efficiency to identify muons in the H1 and ZEUS analyses is $\sim 90\%$ and $\sim 55\%$, respectively. The lower muon identification efficiency for ZEUS is due to a lower trigger efficiency [6].

Multi-lepton events are selected by requiring at least two central ($20^\circ < \theta < 150^\circ$) electron or muon candidates, of which one must have $P_T^\ell > 10$ GeV and the other $P_T^\ell > 5$ GeV. Additional leptons identified in the detector according to the criteria defined above may be present in the event. All lepton candidates are required to be isolated with respect to each other by a minimum distance of at least $0.5$ units in the $\eta - \phi$ plane. No explicit requirement on the charge of the lepton candidates is imposed. Lepton candidates are ordered according to decreasing transverse momentum, $P_T^{\ell_i} > P_T^{\ell_{i+1}}$. According to the number and the flavour of the lepton candidates, the events are classified into mutually exclusive samples.

The production cross section of $e^+e^-$ and $\mu^+\mu^-$ pairs is measured in the photoproduction regime, in which the virtuality $Q^2$ of the photon emitted by the beam lepton is low. Sub-samples of $ee$ and $\mu\mu$ events dominated by photon-photon collisions are selected, labelled $(\gamma\gamma)_e$ and $(\gamma\gamma)_\mu$, respectively. In these subsamples a significant reduction compared to the initial state must be observed in the difference $E - P_z$ of the energy and the longitudinal momentum of all visible particles, $E - P_z < 45$ GeV. This requirement selects events in which the scattered electron is lost in the beampipe and corresponds to a cut on $Q^2 < 1$ GeV$^2$ and on the event inelasticity, $y = (E - P_z)/2E_e^0 < 0.82$, where $E_e^0$ is the electron beam energy.

The combination of the results of the H1 and ZEUS experiments is performed both on the number of observed events and at the cross section level. Distributions of data events and of MC expectations are added bin by bin. Experimental systematic uncertainties are treated as uncorrelated between both experiments. A detailed list of all experimental systematic uncertainties considered by both experiments can be found in the previous publications [5, 6]. A theoretical uncertainty of 3% on the total lepton pair contribution calculated from the GRAPE MC is considered, correlated between the experiments.

Cross sections measured by H1 and ZEUS are combined using a weighted average [10], assuming that the experimental systematic uncertainties are uncorrelated between the H1 and ZEUS experiments.

# 4 Results

## 4.1 Kinematic Distributions

The number of selected events in the data are compared to the SM predictions in Table 1 for the different samples $ee$, $\mu\mu$, $e\mu$, $eee$ and $e\mu\mu$. The observed numbers of events are in good agreement with the SM expectations. The $e\mu\mu$, $\mu\mu$ and $e\mu$ samples are dominated by muon pair production while the $eee$ and $ee$ samples contain mainly events from electron pair production. The NC DIS and QEDC processes give rise to a sizable background contribution in the $ee$ sample where the H1 and ZEUS analyses have slightly different background rejection capabilities. The contribution from NC DIS and QEDC processes to the total SM expectation amounts to 11% for H1, while it is 24% for ZEUS. Most of the events in the $e\mu$ sample arise from muon pair production at high $Q^2$, in which the beam electron is scattered at a large angle in the detector, while one of the muons is outside the acceptance region. In this sample, the NC DIS background contributes to $\sim 10\%$ in both H1 and ZEUS experiments.

The distributions of the invariant mass $M_{12}$ of the two highest $P_T$ leptons for the $eee$ and $e\mu\mu$ samples are shown in Figs. 1(a) and (b), respectively. The distributions of the invariant mass $M_{12}$ of the two leptons in the di-lepton event samples are presented in Figs. 1(c), (d) and (e). An overall agreement with the SM prediction is observed in all cases. High invariant mass events ($M_{12} > 100$ GeV) are observed in the data. The corresponding observed and predicted event yields are summarised for all samples in Table 2. One $ee$ and two $eee$ high mass events are observed by ZEUS [6], while the other high mass events are from the H1 analysis [5]. Compared to the H1 results published in [5], one $eee$ high mass event is not selected in this combined analysis due to the increased electron energy threshold of $E_e > 10$ GeV in the central region. The results for $e^+p$ and $e^-p$ data are also shown separately in Table 2. All high mass events are observed by both experiments in $e^+p$ collisions only.

Figure 2 presents the distributions of $\sum P_T$ of the observed multi-lepton events compared to the SM expectation. Good overall agreement between the data and the SM prediction is observed. For $\sum P_T > 100$ GeV, seven events are observed in total, compared to $3.13 \pm 0.26$ expected from the SM (see Table 3). These seven events were all recorded in the $e^+p$ data, for which the SM expectation is $1.94 \pm 0.17$. The events correspond to the four $ee$ and the two $e\mu\mu$ events observed with $M_{12} > 100$ GeV, together with one $eee$ event observed with $M_{12} = 93$ GeV.

## 4.2 Cross Section Measurements

Total visible and differential cross sections for di-electron and di-muon production from photon-photon collisions are measured using the selected $(\gamma\gamma)_e$ and $(\gamma\gamma)_\mu$ samples. The kinematic domain of the measurement is defined by $20^\circ < \theta^{\ell_{1,2}} < 150^\circ$, $P_T^{\ell_1} > 10$ GeV, $P_T^{\ell_2} > 5$ GeV, $Q^2 < 1$ GeV$^2$ and $y < 0.82$. The data samples at $\sqrt{s} = 301$ GeV and 319 GeV are combined taking into account their respective luminosities. Assuming a linear dependence of the cross section on the proton beam energy, as predicted by the SM, the resulting cross section corresponds to an effective $\sqrt{s} = 318$ GeV. The effect of final state radiation on the cross section was checked and found to be negligible. The total numbers of observed $(\gamma\gamma)_e$ and $(\gamma\gamma)_\mu$ events are in agreement with the SM expectations, as summarised in Table 1. In the $(\gamma\gamma)_e$ sample, the contamination from NC DIS and QEDC background events is 2%. No significant background is present in the $(\gamma\gamma)_\mu$ sample.

The cross section is evaluated in each bin $i$ using the formula

$$\sigma_i = \frac{N_i^{\mathrm{data}} - N_i^{\mathrm{bgr}}}{\mathcal{L} \cdot A_i}, \tag{1}$$

where $N_i^{\mathrm{data}}$ is the number of observed events in bin $i$, $N_i^{\mathrm{bgr}}$ the expected contribution from background processes in bin $i$, $\mathcal{L}$ the integrated luminosity of the data and $A_i$ the signal acceptance in bin $i$. The signal acceptance is calculated using the GRAPE MC events, as the ratio of the number of events reconstructed in bin $i$ divided by the number of events generated in the same bin. For $ep \rightarrow e\, e^+e^-X$ events, the mean signal acceptances in the H1 and ZEUS experiments are 45% and 60%, respectively. In case of $ep \rightarrow e\, \mu^+\mu^-X$ events, it is 60% for H1 and 30% for ZEUS.

Differential cross sections of lepton pair production as a function of the transverse momentum of the leading lepton $P_T^{\ell_1}$ and of the invariant mass of the lepton pair $M_{\ell\ell}$ are shown in Fig. 3 for the combined electron and muon samples. The measurements are in good agreement with the SM cross sections.

# 5 Conclusion

The production of multi-lepton (electron or muon) events at high transverse momenta is studied using the full $e^{\pm}p$ data sample collected by the H1 and ZEUS experiments at HERA. It corresponds to a total integrated luminosity of $0.94$ fb$^{-1}$. The yields of di-lepton and tri-lepton events are in good agreement with the SM predictions. In each sample distributions of the invariant mass $M_{12}$ of the two highest $P_T$ leptons and of the scalar sum of the lepton transverse momenta $\sum P_T$ are in good overall agreement with the SM expectation.

In di-lepton and tri-lepton samples, a total of twelve events are observed with invariant masses $M_{12}$ above $100$ GeV, a region where the SM expectation is low. Seven events have a $\sum P_T > 100$ GeV, whereas the corresponding SM expectation for $e^+p$ collisions is $1.94 \pm 0.17$. This observation corresponds to a significance of $2.6\sigma$. All high mass and high $\sum P_T$ events are observed by both experiments in $e^+p$ collisions only, while, for comparable SM expectations, none are observed in $e^-p$ collisions.

The total and differential cross sections for electron and muon pair production are measured in a restricted phase space dominated by photon-photon interactions. The measured cross sections are in agreement with the SM predictions.

# References


[1] J. A. M. Vermaseren, "Two Photon Processes At Very High-Energies," Nucl. Phys. B **229** (1983) 347.

[2] A. Aktas *et al.* [H1 Collaboration], "Search for doubly-charged Higgs boson production at HERA," Phys. Lett. B **638** (2006) 432 [hep-ex/0604027].

[3] A. Aktas *et al.* [H1 Collaboration], "Multi-electron production at high transverse momenta in e p collisions at HERA," Eur. Phys. J. C **31** (2003) 17 [hep-ex/0307015].

[4] A. Aktas *et al.* [H1 Collaboration], "Muon pair production in e p collisions at HERA," Phys. Lett. B **583** (2004) 28 [hep-ex/0311015].

[5] F. D. Aaron *et al.* [H1 Collaboration], "Multi-Lepton Production at High Transverse Momenta in ep Collisions at HERA," Phys. Lett. B **668** (2008) 268 [0806.3987 [hep-ex]].

[6] XXXXX *et al.* [ZEUS Collaboration], "Multi-lepton production at high transverse momentum at HERA," Submitted to ??.

[7] I. Abt *et al.* [H1 Collaboration], "The H1 detector at HERA," Nucl. Instrum. Meth. A **386** (1997) 310;
I. Abt *et al.* [H1 Collaboration], "The Tracking, calorimeter and muon detectors of the H1 experiment at HERA," Nucl. Instrum. Meth. A **386** (1997) 348.

[8] ZEUS Collaboration, U. Holm (ed.), *the ZEUS Detector*. Status Report (unpublished), DESY (1993), available on http://www-zeus.desy.de/bluebook/bluebook.html.

[9] T. Abe, GRAPE-Dilepton version 1.1, Comput. Phys. Commun. **136** (2001) 126 [hep-ph/0012029].

[10] C. Amsler *et al.* [Particle Data Group], “Review of particle physics,” Phys. Lett. B **667** (2008) 1.

| H1+ZEUS Multi-Lepton analysis HERA I+II ($0.94$ fb$^{-1}$, preliminary) | | | | |
|---|---|---|---|---|
| Selection | Data | SM | Pair Production (GRAPE) | NC DIS + QEDC |
| $ee$ | 873 | $895 \pm 57$ | $724 \pm 41$ | $171 \pm 28$ |
| $\mu\mu$ | 298 | $320 \pm 36$ | $320 \pm 36$ | $< 0.5$ |
| $e\mu$ | 173 | $167 \pm 10$ | $152 \pm 9$ | $14.5 \pm 2.8$ |
| $eee$ | 116 | $117 \pm 7$ | $116.5 \pm 6.5$ | $0.5 \pm 0.3$ |
| $e\mu\mu$ | 140 | $147 \pm 15$ | $147 \pm 15$ | $< 0.5$ |
| $(\gamma\gamma)_e$ | 284 | $293 \pm 18$ | $290 \pm 18$ | $4.2 \pm 1.3$ |
| $(\gamma\gamma)_\mu$ | 235 | $247 \pm 26$ | $247 \pm 26$ | $< 0.5$ |

Table 1: Observed and predicted event yields for the different event samples. The errors on the predictions include model uncertainties and experimental systematic errors added in quadrature. The limits on the background estimations correspond to the selection of no event in the simulated sample and are quoted at 95% confidence level.

| H1+ZEUS Multi-Lepton analysis HERA I+II ($0.94$ fb$^{-1}$, preliminary) | | | | |
|---|---|---|---|---|
| $M_{12}$ >100 GeV | | | | |
| Selection | Data | SM | Pair Production (GRAPE) | NC DIS + QEDC |
| All data ($0.94$ fb$^{-1}$) | | | | |
| $ee$ | 4 | $2.98 \pm 0.28$ | $1.69 \pm 0.15$ | $1.29 \pm 0.16$ |
| $\mu\mu$ | 1 | $0.55 \pm 0.12$ | $0.55 \pm 0.12$ | $< 0.01$ |
| $e\mu$ | 1 | $0.65 \pm 0.07$ | $0.64 \pm 0.06$ | $< 0.02$ |
| $eee$ | 4 | $1.27 \pm 0.12$ | $1.27 \pm 0.12$ | $< 0.03$ |
| $e\mu\mu$ | 2 | $0.31 \pm 0.06$ | $0.31 \pm 0.06$ | $< 0.01$ |
| $e^+p$ collisions ($0.56$ fb$^{-1}$) | | | | |
| $ee$ | 4 | $1.68 \pm 0.18$ | $0.94 \pm 0.11$ | $0.74 \pm 0.12$ |
| $\mu\mu$ | 1 | $0.32 \pm 0.08$ | $0.32 \pm 0.08$ | $< 0.01$ |
| $e\mu$ | 1 | $0.40 \pm 0.05$ | $0.39 \pm 0.05$ | $< 0.02$ |
| $eee$ | 4 | $0.79 \pm 0.09$ | $0.79 \pm 0.09$ | $< 0.03$ |
| $e\mu\mu$ | 2 | $0.16 \pm 0.04$ | $0.16 \pm 0.04$ | $< 0.01$ |
| $e^-p$ collisions ($0.38$ fb$^{-1}$) | | | | |
| $ee$ | 0 | $1.25 \pm 0.13$ | $0.71 \pm 0.11$ | $0.54 \pm 0.08$ |
| $\mu\mu$ | 0 | $0.23 \pm 0.10$ | $0.23 \pm 0.10$ | $< 0.01$ |
| $e\mu$ | 0 | $0.26 \pm 0.03$ | $0.25 \pm 0.03$ | $< 0.02$ |
| $eee$ | 0 | $0.49 \pm 0.74$ | $0.49 \pm 0.07$ | $< 0.03$ |
| $e\mu\mu$ | 0 | $0.14 \pm 0.05$ | $0.14 \pm 0.05$ | $< 0.01$ |

Table 2: Observed and predicted multi-lepton event yields for masses $M_{12} > 100$ GeV for the different event samples in all analysed samples. The errors on the predictions include model uncertainties and experimental systematic errors added in quadrature. The limits on the background estimations correspond to the selection of no event in the simulated sample and are quoted at 95% confidence level.

| H1+ZEUS Multi-Lepton analysis HERA I+II ($0.94$ fb$^{-1}$, preliminary) | | | | |
|---|---|---|---|---|
| $\sum P_T$ >100 GeV | | | | |
| Data sample | Data | SM | Pair Production (GRAPE) | NC DIS + QEDC |
| e$^+$p ($0.56$ fb$^{-1}$) | 7 | $1.94 \pm 0.17$ | $1.52 \pm 0.14$ | $0.42 \pm 0.07$ |
| e$^-$p ($0.38$ fb$^{-1}$) | 0 | $1.19 \pm 0.12$ | $0.90 \pm 0.10$ | $0.29 \pm 0.05$ |
| All ($0.94$ fb$^{-1}$) | 7 | $3.13 \pm 0.26$ | $2.42 \pm 0.21$ | $0.71 \pm 0.10$ |

Table 3: Observed and predicted multi-lepton event yields for $\sum P_T > 100$ GeV. Di-lepton and tri-lepton events are combined. The errors on the predictions include model uncertainties and experimental systematic errors added in quadrature.

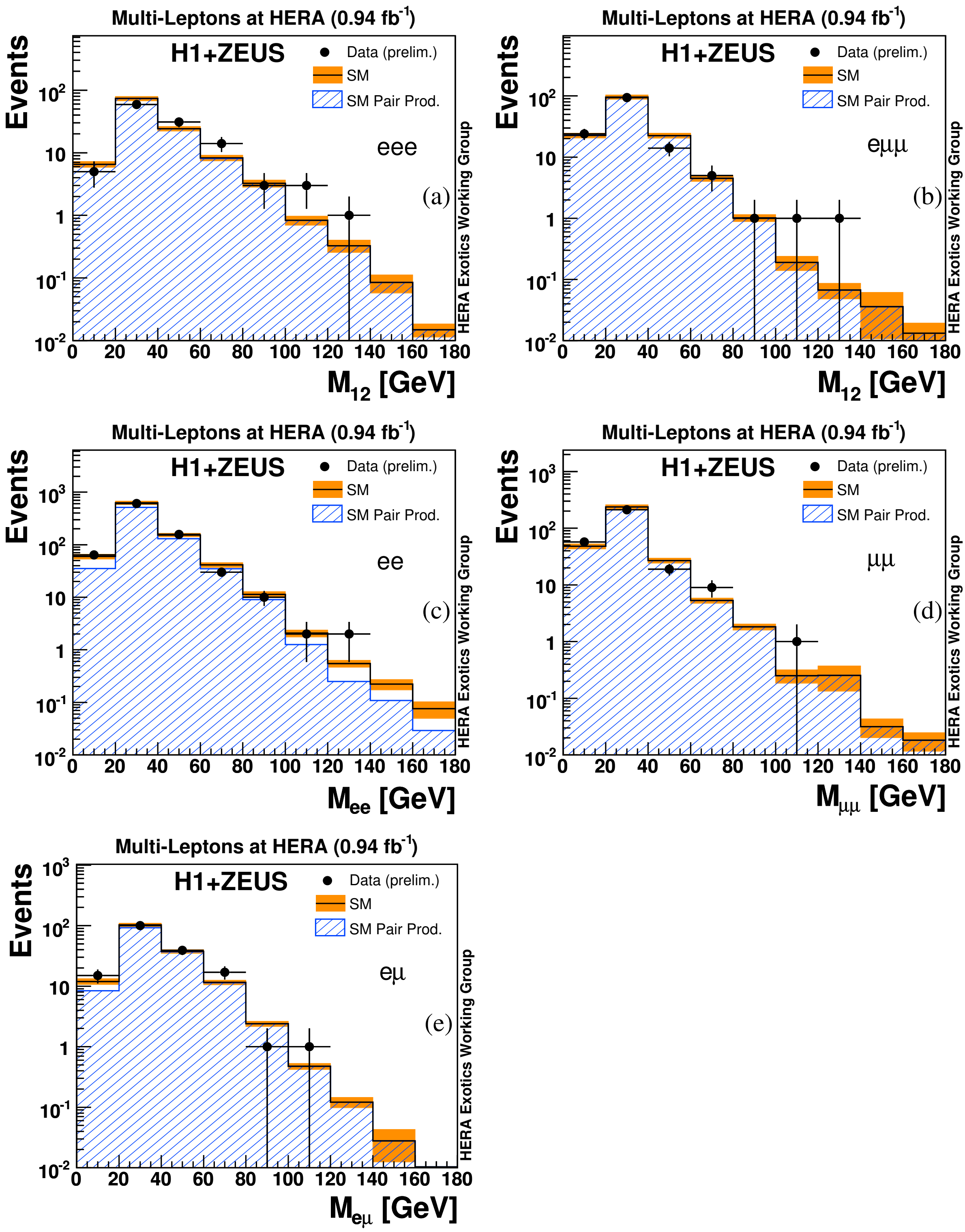


Figure 1: The distribution of the invariant mass of the two highest $P_T$ leptons for events classified as $eee$ (a), $e\mu\mu$ (b) and $ee$ (c), $\mu\mu$ (d) and $e\mu$ (e). The points correspond to the observed data events and the open histogram to the SM expectation. The total error on the SM expectation is given by the shaded band. The component of the SM expectation arising from lepton pair production is given by the hatched histogram.

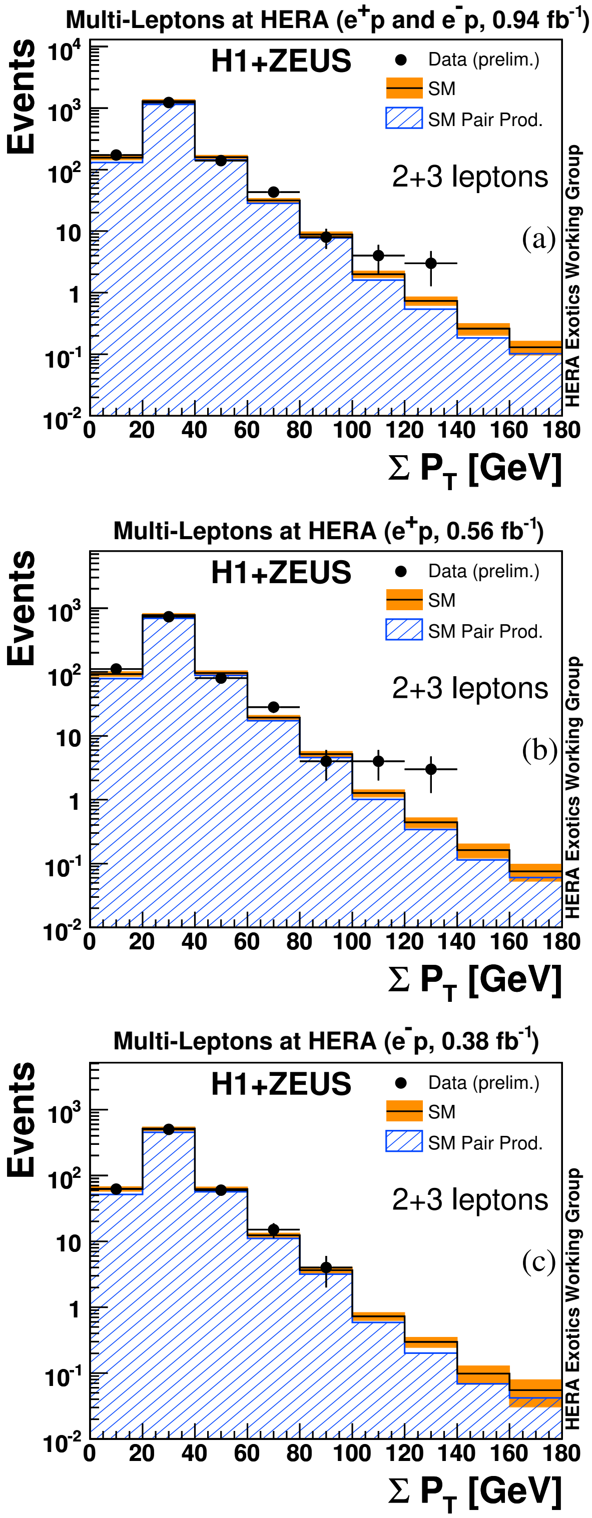


Figure 2: The distribution of the scalar sum of the transverse momenta $\sum P_T$ for combined di-lepton and tri-lepton event samples for all data (a) as well as for $e^+p$ (b) and $e^-p$ (c). The points correspond to the observed data events and the open histogram to the SM expectation. The total error on the SM expectation is given by the shaded band. The component of the SM expectation arising from lepton pair production is given by the hatched histogram.

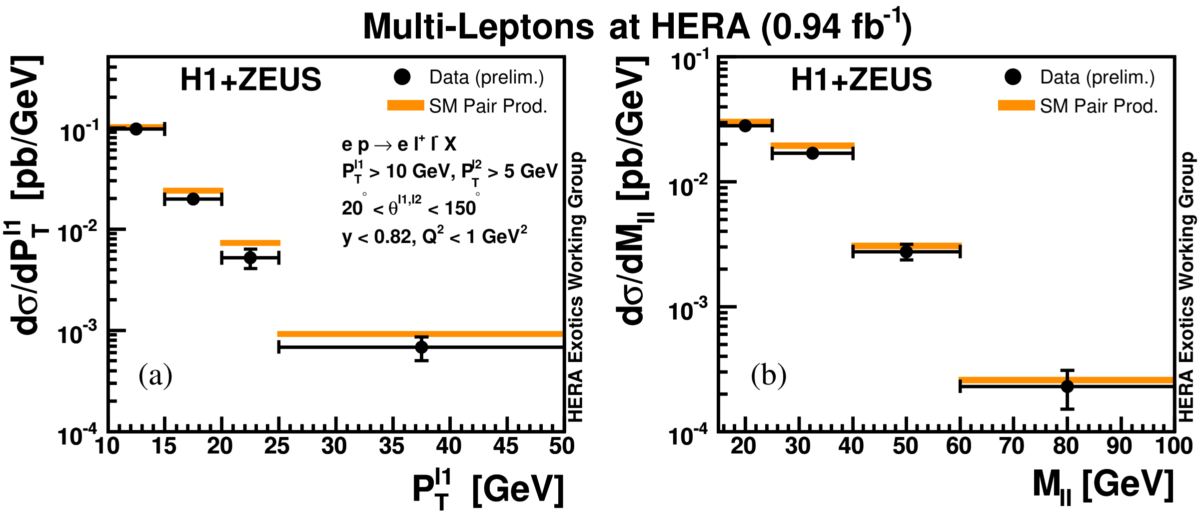


Figure 3: The measured cross section for lepton pair production in a restricted phase space dominated by the photon-photon process as a function of the leading lepton transverse momentum $P_T^{\ell_1}$ (a) and the invariant mass of the lepton pair $M_{\ell\ell}$ (b). The differential cross section is averaged over the intervals shown. The inner error bars represent the statistical errors, the outer error bars the statistical and systematic errors added in quadrature. The bands represent the one standard deviation uncertainty in the SM prediction.